Thermochimica Acta, 49 (1981) 319—331
Elsevier Scientific Publishing Company, Amsterdam — Printed in Belgium

THERMODYNAMIC PROPERTIES OF 50 MOLE% $NaNO_3$—50% KNO_3 (HTS_2)

MASAYUKI KAMIMOTO

Energy Division, Electrotechnical Laboratory, Sakura-mura, Niihari-gun. Ibaraki (Japan)

(Received 7 May 1981)

ABSTRACT

The mechanism of formation of the solid solution, phase separation, and the formation of the eutectic mixture were investigated by DSC and X-ray diffraction for 50 mole% $NaNO_3$—50% KNO_3 (HTS_2), and its enthalpy change was measured from 25 to 450°C by a high-temperature calorimeter of the twin type. Based on the enthalpy change measured, the relation between the thermodynamic properties and the phase diagram of the $NaNO_3$—KNO_3 system is discussed assuming the regular solution approximation.

INTRODUCTION

Several mixtures of alkali nitrates and nitrites have low melting temperatures. For example, a eutectic mixture containing 40 wt.% $NaNO_2$, 7 wt.% $NaNO_3$, and 53 wt.% KNO_3 melts at 142°C [1] and has been used, for a long time, as a heat transfer medium because of its low cost and good compatibility with common structural materials. This mixture is called HTS (Heat Transfer Salt), HTS_1, or Hitec (Du Pont trade name) because of its use for heat transfer. It can also be used for sensible heat storage. For example, the application of this mixed salt to thermal storage, for load leveling, and for solar thermal electric power generation were postulated to be promising [2].

Another mixture, 50 mole% $NaNO_3$—50 mole% KNO_3, which is sometimes called HTS_2 or draw salt, has a higher melting temperature (222°C) than HTS_1. Although a low melting temperature is preferable for heat transfer and sensible heat storage, HTS_2 is more promising from the viewpoints of cost and thermal stability [2].

So far, there exist only a few data on the thermodynamic properties of HTS_2 in spite of its importance. The reported values of the heat of fusion [3—6] are not in good agreement with each other and neither are the values of heat capacity [3,4]. Furthermore, the heat capacity of the liquid phase measured by Voskresenskaya et al. [4] shows a large negative temperature coefficient, while that by Nguyen-Duy and Dancy [3] shows no temperature dependence.

Several investigations of the phase diagram of the $NaNO_3$—KNO_3 system [7—10] indicate that the system has a minimum melting point at a composition of 50 mole% KNO_3, i.e. HTS_2. It forms a solid solution below the

0040-6031/81/0000—0000/$02.50

solidus and phase separation followed by formation of a eutectic mixture occurs in a lower temperature range [7,9].

Since slow diffusion rates of atoms and ions are expected in such a low temperature range, these phenomena might not completely occur at some cooling rates. The thermal behavior of HTS_2 and its enthalpy change obtained by drop methods, in which the temperature of a sample is quickly changed, might therefore be influenced by the thermal history of HTS_2.

In the present study, the effect of the thermal history has been investigated by DSC and X-ray diffraction and the enthalpy change has been measured for quenched and annealed samples of 50 mole% $NaNO_3$—50 mole% KNO_3 by a high-temperature calorimeter of the twin type. Based on the enthalpy change measured, the relation between the thermodynamic properties and the phase diagram is discussed assuming the regular solution approximation.

EXPERIMENTAL

Samples

Chemically pure $NaNO_3$ and KNO_3 purchased from Wako Pure Chemical Industries, Ltd. were used for making the equimolar mixture. For the enthalpy change measurement, the reagents were first heated up to about 130°C in order to dry them and were quickly weighed in air to give an equimolar ratio and they were put into a gold sample container of 8 mm outer diameter and length 45 mm. The specimen was again dried in air at about 130°C and the container was then sealed by arc melting.

Apparatus and measurements

DSC measurement was made under dry nitrogen flow using model No. 8085 of Rigaku Denki Co., Ltd. and Perkin Elmer DSC-2. A platinum sample pan was used for both.

X-Ray diffraction patterns at room temperature and at about 200°C were obtained with a θ—θ diffractometer made by Rigaku Denki Co. Ltd., the X-ray source and the detector of which rotate around a sample in a vertical plane. MoK_α radiation was used and the beam was monochromated by a bent graphite monochrometer. The sample temperature was measured by a platinum/platinum—rhodium (13%) thermocouple, which was inserted into the sample loaded in the platinum container.

The enthalpy change measurement was performed by the drop method using a high-temperature calorimeter of the twin type. The details of the calorimeter were given in an earlier paper [11].

A sample container containing the equimolar mixture, one containing the N.B.S. standard sapphire, and one without any sample (blank) were prepared as are listed in Table 1. These containers were kept at the required temperature between 25 and 450°C in a small furnace placed above the calorimeter for at least 1 h after a steady state was attained, and then

TABLE 1

Masses of specimens and containers

Specimen	Mass (g)	
	Specimen	Container
Sapphire	3.4290	4.8735
HTS_2	1.9926	5.0802
Blank		4.6987

dropped into the calorimeter maintained below or above the melting temperature of HTS_2 (222°C). These operation temperatures were 198.6 and 228.5°C.

The apparatus constant, A, is defined as $\int \Delta T \, dt/Q$, where the numerator is the time integral of the differential temperature between a calorimeter cell and an isothermal jacket and the denominator is the heat change in the calorimeter cell. It was determined from enthalpy changes observed when the gold sample container with the standard sapphire and the blank were dropped from room temperature to either of the operation temperatures. The determined apparatus constants are plotted in Fig. 1 against the operation temperature of the calorimeter together with the previously published data [11] at the operation temperatures of 25, 300, and 400°C. Although there is a somewhat large temperature dependence, it has no serious effect on the measurements because the temperature of the calorimeter is controlled within ±0.3°C during all the measurements.

In order to ascertain the accuracy of the measurements by using the apparatus constants at 198.6 and 228.5°C determined as mentioned above, the values of the enthalpy change of the N.B.S. standard sapphire were obtained over the temperature range between 25 and 450°C. The values obtained showed ±1.5% deviation from the literature values [12].

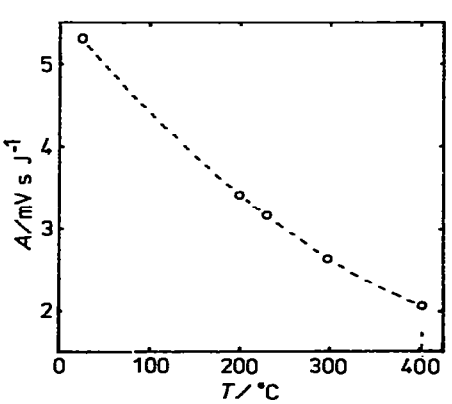

Fig. 1. Apparatus constant of the calorimeter.

RESULTS AND DISCUSSION

Preliminary DSC measurement

For a preliminary examination of the thermal behavior of HTS_2, DSC measurements were carried out between 50 and 250°C at heating and cooling rates of 2.5°C min^{-1}. For the measurements, $NaNO_3$ and KNO_3 as received were put into a platinum sample pan in equimolar ratio.

Figure 2 shows the DSC curves obtained. After the first melting, the sample was held at 250°C for 30 min and then cooled down to 50°C (first cooling). The sample was held at 50°C for 30 min and again heated up to 250°C (second heating). This heating-and-cooling cycle was repeated three times. Only two cycles, however, are shown in the figure since the third heating and cooling curves were the same as the second.

The reason for the deformed shape of the first endothermic peak of the fusion is that the starting materials were not homogeneously mixed. Both peaks of fusion and crystallization were reasonably sharp after the first melting because of the homogeneous mixing of $NaNO_3$ and KNO_3.

The endothermic peak observed at 129°C in the first heating is attributed to the phase transition of KNO_3. It is well known that this transition is separated into two transitions at 123 and 113°C in the cooling mode [13]. These transitions were not observed in the cooling curves and a quite small peak was observed between 80 and 95°C. In the second and third heating curves, the peak at 129°C disappears and a small peak appears between 70 and 100°C.

As already mentioned, HTS_2 forms a solid solution below the solidus. According to the phase diagram determined by Kofler [9], which is shown in Fig. 3, and that by Jänecke [7], this solid solution begins to separate into two other solid solutions of different compositions at a lower temperature,

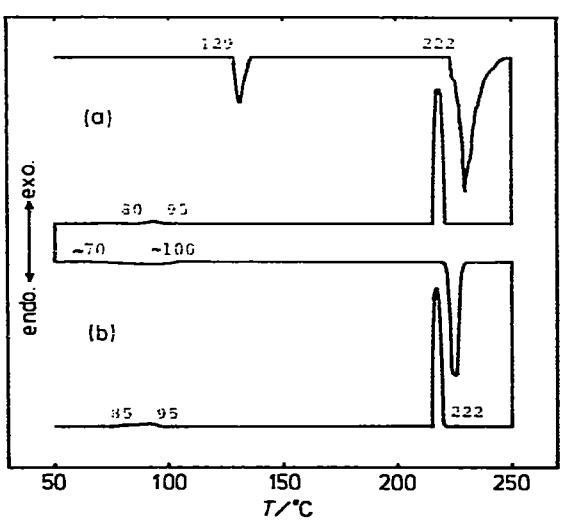

Fig. 2. DSC curves of heating and cooling cycles of HTS_2. (a) The first cycle for the specimen without being mixed before heating; (b) the second cycle.

which is reported to be 180°C by Jänecke [7] and 165°C by Kofler [9]. Jänecke also reported the formation of a eutectic mixture at 89°C, while Kofler reported 105°C as a eutectic temperature. No peak was observed around 180 and 165°C in our DSC measurements. Small peaks observed near 100°C seems to correspond to the formation of the eutectic mixture.

It is, however, not clear from this experiment alone whether the solid phases formed in this heating-and-cooling cycle are in equilibrium states as shown in the phase diagram of the $NaNO_3$—KNO_3 system. The following DSC and X-ray diffraction measurements were performed for a more detailed examination of the thermal behavior of HTS_2.

Formation of the solid solution below the melting temperature

To investigate the formation of the solid solution below the melting temperature [7,9], DSC measurement was done between 200 and 250°C at a rate of 2.5°C min^{-1}. The specimen kept at 250°C for 30 min was cooled and annealed at 200°C for a certain time less than 24 h and then again heated up to 250°C. Nine cycles were made and the heat of fusion was calculated for each peak in the heating mode.

Figure 4 shows the DSC peaks of the fusion for two cases. The peak shape without annealing at 200°C [(a) in the figure] is not so sharp as that obtained after annealing for 24 h [(b) in the figure]. Nevertheless, the heat of fusion is almost the same: 97 and 100 J g^{-1} for cases (a) and (b), respectively. For every other case in which the annealing time at 200°C was between the two cases, the heat of fusion measured was the same within experimental error.

From these observations, the rapid formation of the solid solution in this temperature range was expected and X-ray diffraction analysis was done at 200 ±10°C to confirm it.

The sample of the equimolar mixture was prepared by a natural cooling of the melt in the platinum container and then heated from room temperature to about 200°C for 30 min. Subsequently, the pattern of the mixture [(c) in

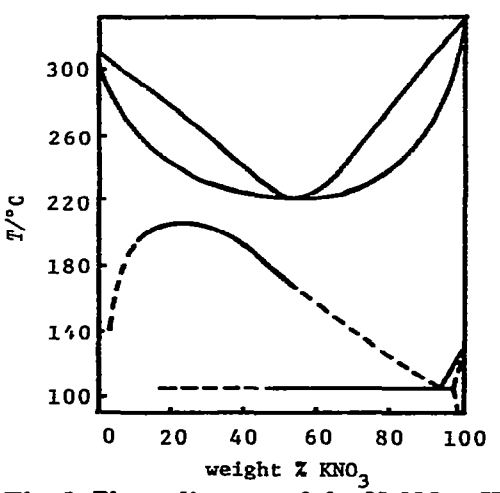

Fig. 3. Phase diagram of the $NaNO_3$—KNO_3 system determined by Kofler.

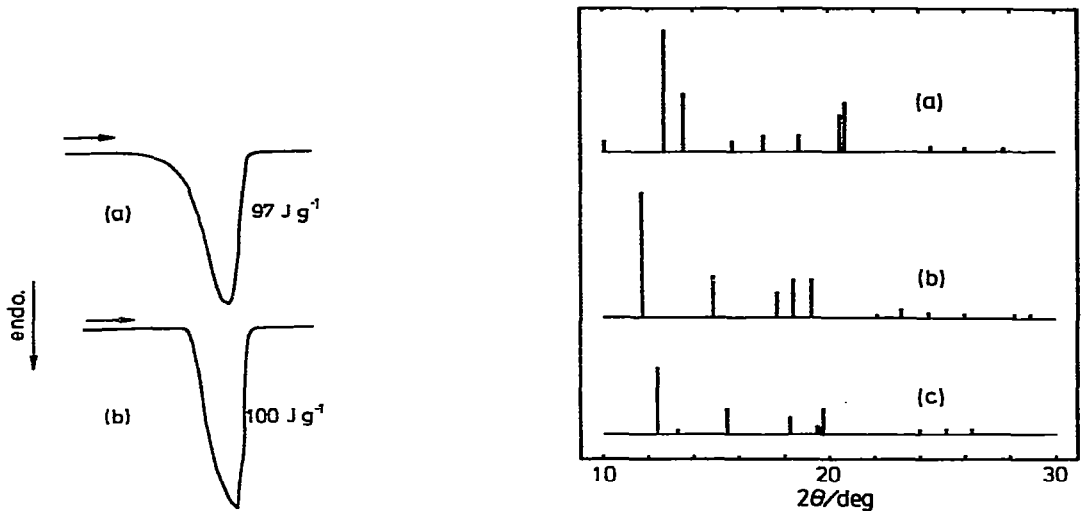

Fig. 4. DSC peaks due to fusion of HTS_2 in the heating mode. (a) Without annealing at 200°C; (b) after annealing at 200°C for 24 h.

Fig. 5. X-Ray diffraction patterns at 200 ± 10°C. The lines show a peak position and relative logarithmic peak height. (a) $NaNO_3$; (b) KNO_3; (c) HTS_2.

Fig. 5] was obtained at about 200°C, and it is different from the pattern of either $NaNO_3$ [(a) in the figure] or KNO_3 [(b) in the figure] at 200°C. The rapid formation of the solid solution below the melting temperature was thus confirmed.

Phase separation and formation of the eutectic mixture

To examine whether HTS_2 cooled down to 50°C at a rate of 2.5°C min^{-1} is in an equilibrium state or not, DSC and X-ray diffraction at room temperature were carried out for the following three samples of HTS_2.

(1) A quenched sample. The equimolar mixture was melted and cooled by blowing air (quenched) in a platinum sample container for X-ray diffraction.

(2) A quenched-and-ground sample. About 20 g of the equimolar mixture was melted and cooled by blowing air (quenched) and then it was ground into powder.

(3) An annealed sample. The quenched-and-ground sample was annealed at room temperature in a sealed pyrex tube for one month.

At first, X-ray diffraction patterns of the annealed and the quenched samples were obtained at room temperature together with the patterns of $NaNO_3$ and KNO_3. Although the peaks shift, most of the peaks of both $NaNO_3$ [(a) in Fig. 6] and KNO_3 [(b) in the figure] appear in the pattern of the annealed sample [(c) in the figure]. On the other hand, the quenched sample shows a very strong peak at $2\theta \sim 12.5°$, which does not exist in the pattern of the annealed sample.

Since the quenched sample is not powder, a particular peak might become very strong due to some orientation of the crystal. Considering a probable effect of the orientation, two quenched and ground samples were then prepared for X-ray diffraction. One of the quenched-and-ground mixtures [(d)

in Fig. 6] shows almost the same pattern as the annealed sample whereas the other quenched-and-ground mixture [(e) in the figure] shows a strong peak at $2\theta \sim 12.8°$ C.

To thermally observe the difference among these samples, DSC curves were obtained for the quenched-and-ground and the annealed samples. Figure 7 shows the heating curves for these samples. It should be noted that the small endothermic peak around 100°C, which is seen in Fig. 2, shifts to higher temperatures and its area becomes larger in these cases.

This fact seems to show that the sample of HTS_2 cooled at a rate of 2.5°C min^{-1} does not reach a thermodynamically stable state. That is in accord with the X-ray observations, i.e. a strong peak near $2\theta = 12.5 \sim 12.8°$ exists in the pattern of the quenched sample and it disappears by annealing and sometimes by grinding.

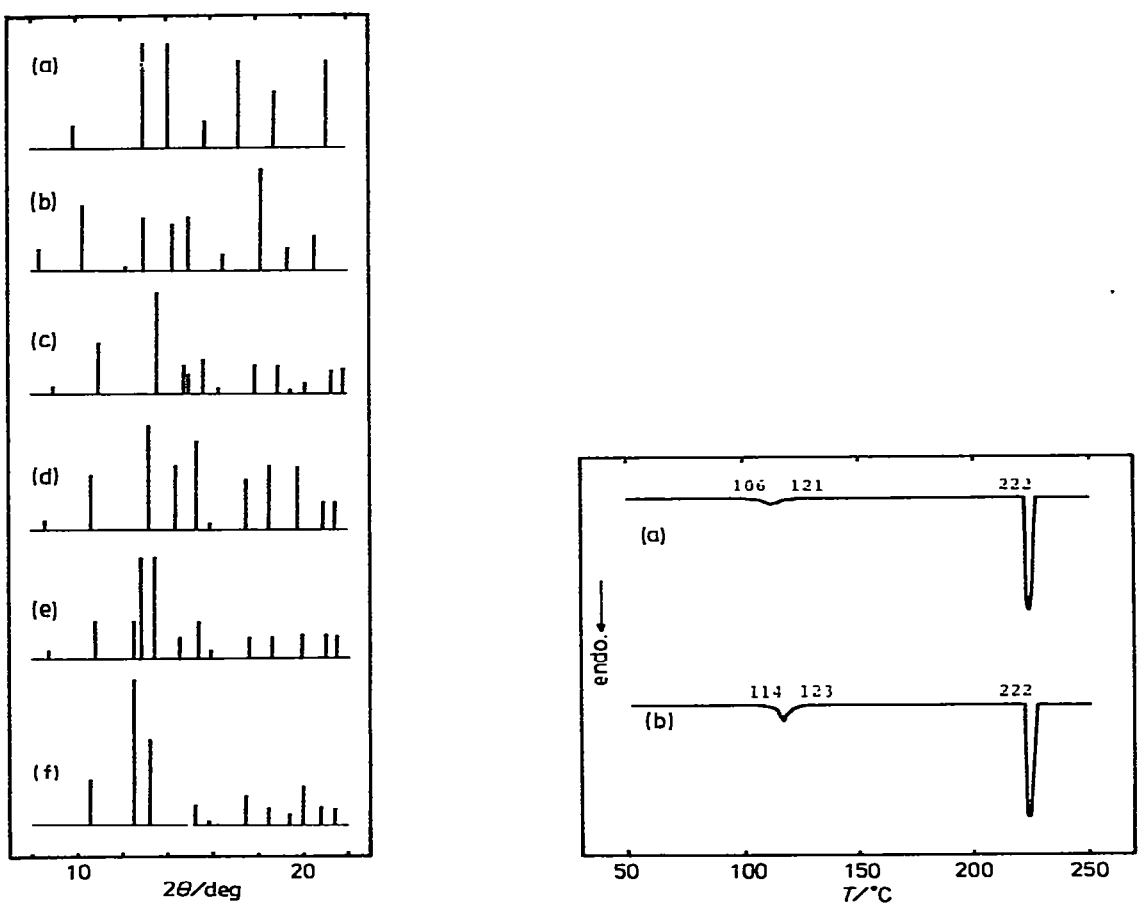

Fig. 6. X-Ray diffraction patterns at room temperature. The lines show a peak position and relative logarithmic peak height. (a) $NaNO_3$; (b) KNO_3; (c) the annealed sample of HTS_2; (d) and (e) quenched-and-ground sample of HTS_2; (f) the quenched sample of HTS_2.

Fig. 7. DSC heating curves of HTS_2. (a) The quenched-and-ground sample; (b) the annealed sample.

The annealed sample shows a pattern including most of the peaks of $NaNO_3$ and KNO_3. That is not inconsistent with the absence of the DSC peaks of the transitions of KNO_3 after a melting of the mixture, since one of the solid solutions which exist near room temperature in equilibrium is very close to KNO_3 in composition and lattice spacings.

Therefore, it would be reasonable that there exist at least three solid phases, i.e. the quenched phase, s-I, below 100°C, the annealed phase, s-II, below 100°C, and the solid solution, s-III, below 222°C. The solid phase s-II is more stable than s-I. More precise X-ray diffraction analysis is necessary to characterize these solid phases.

Enthalpy change measurement

The standard enthalpy change values, $h_T^0 - h_{298}^0$, were obtained from the measured enthalpy change data and they are plotted in Fig. 8. The open circles are the data when the operation temperature of the calorimeter was 198.6°C, whereas the open triangles are those at the operation temperature of 228.5°C. After one measurement at a temperature, the dropped specimen was picked up from the calorimeter cell and annealed overnight for the next measurement in the upper furnace controlled at a preset temperature. Below 100°C, it was annealed for at least a few days. It can be seen that the open circles and the open triangles lie on the same linear lines both in the liquid phase and in the solid phase except for the temperature range between 100 and 150°C. A scattering of the data was observed between 100 and 150°C.

The solid triangles show the data obtained as follows. After previous measurements, the dropped specimen was picked up and naturally cooled down in air for about 1 h and the measurement was carried out after maintaining the specimen at a preset temperature below 100°C in the upper furnace for about 2 h. The data shown by the solid triangles are considerably higher than the others, and the difference of the data should be due only to a difference in the thermal history. Therefore, the data shown by the solid triangles seem to be for a quenched phase.

Thermodynamic properties

The smoothed standard enthalpy change was determined by assuming a polynomial temperature dependence for each stable phase. A linear temperature dependence was enough to represent the measured enthalpy change values. The best-fit equations are

$$(h_T^0 - h_{298}^0)/\mathrm{J\ g^{-1}} = 1.0666(T/\mathrm{K}) - 318.01 \qquad \text{(s-I, 25—100°C)}$$

$$(h_T^0 - h_{298}^0)/\mathrm{J\ g^{-1}} = 1.3637(T/\mathrm{K}) - 368.83 \qquad \text{(s-III, 150—222°C)}$$

and

$$(h_T^0 - h_{298}^0)/\mathrm{J\ g^{-1}} = 1.4555(T/\mathrm{K}) - 312.86 \qquad \text{(l, 222—450°C)}$$

where l represents liquid phase. In Table 2 are listed the values of the enthalpy of fusion and the heat capacities together with the literature values.

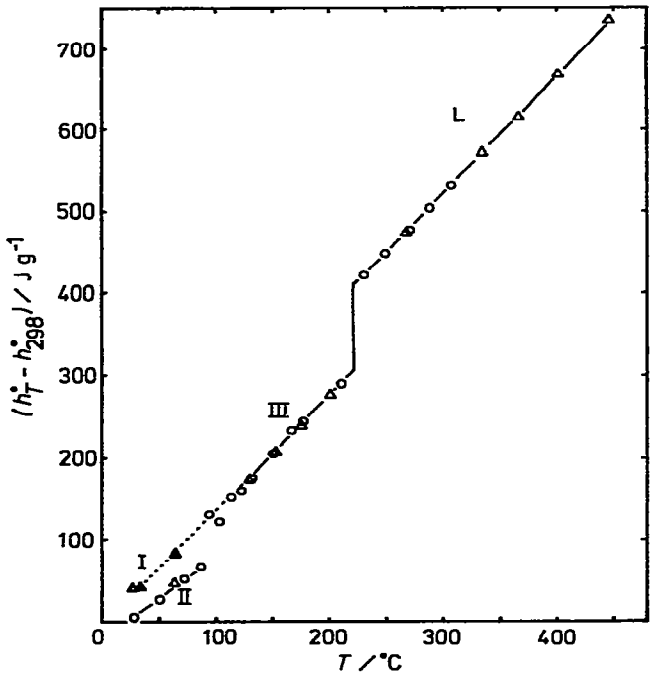

Fig. 8. Standard specific enthalpy change of HTS_2. ○, Data when the operation temperature was 198.6°C; △, data when the operation temperature was 228.5°C; ▲, data for the quenched specimen.

The values determined in this study are in good agreement above 150°C with those by Nguyen-Duy and Dancy [3]. ΔH_m measured by Marchidan and Telea [6] seems too high, and the C_p values determined by Voskresenskaya et al. [4] are higher in the liquid phase and lower in the solid phase than other data.

TABLE 2

Enthalpy of fusion and heat capacity of HTS_2

	ΔH_m/kJ mole^{-1}	C_p/kJ mole^{-1} K^{-1}	Temp. range/°C
This work	9.46	0.0992 (s-II)	25—100
		0.127 (s-III)	150—222
		0.136 (l)	222—450
Nguyen-Duy and Dancy [3]	10.5	0.132 (s)	177—222
		0.142 (l)	222—327
Voskresenskaya et al. [4]	10.5	0.112 (s)	110.0
		0.115 (s)	210.2
		0.156 * (l)	222—450 (average)
Venkatesetty and Lefrois [5]	9.12		
Marchidan and Telea [6]	13.4		

* An average value in the temperature range.

As shown in the present study, the enthalpies of both annealed and quenched solid phases could be measured by a transposed temperature drop method. It is preferable for determining the thermodynamic functions of materials which are easily quenched by a usual drop method, where a sample is always dropped to a calorimeter at room temperature or 0°C.

Relation between the heat capacity of HTS_2 and those of $NaNO_3$ and KNO_3

Many data on the thermodynamic properties of $NaNO_3$ and KNO_3 have been reported and the most reliable values of the heat capacity in the liquid phase are 0.155 and 0.136 kJ mole^{-1} K^{-1}, respectively [18]. The heat capacity of the liquid phase equimolar mixture obtained in this study is 0.136 kJ mole^{-1} K^{-1} and it approximately equals the simple average of these values, 0.146 kJ mole^{-1} K^{-1}. Thus, the Kopp—Neumann law of molar additivity [14] roughly holds for the heat capacity of liquid-phase HTS_2.

The heat capacities averaged between 25 and 100°C for solid $NaNO_3$ and KNO_3 are 0.098 and 0.100 kJ mole^{-1} K^{-1} [15], respectively, and the molar average of them is the same as the measured value of HTS_2 in the state of the solid II, 0.099 kJ mole^{-1} K^{-1}. The fact is reasonable if the solid II is considered to be in a stable state.

Calculation of the phase diagram

In order to confirm consistency in the thermodynamic properties determined in the present study and the phase diagram of the $NaNO_3$—KNO_3 system, the solidus and the liquidus were calculated. As already pointed out, reliable values of the thermodynamic properties are available for $NaNO_3$ and KNO_3. The enthalpy of mixing of the liquid $NaNO_3$—KNO_3 is reported to be well represented [16] by

$$\Delta H^{mix}/\text{cal mole}^{-1} = x(1-x)\,(-408-68x)$$

in which x is the mole fraction of KNO_3. This equation shows that this binary system is approximately a regular solution in the liquid phase.

Assuming the regular solution approximation also in the solid solution of this system, the liquidus and the solidus can be readily calculated from the simultaneous equations [17]

$$\ln\frac{\gamma_A^s x_A^s}{\gamma_A^l x_A^l} = -\frac{\Delta H_A}{R}\left(\frac{1}{T_A}-\frac{1}{T}\right)-\frac{\Delta C_A}{R}\left(\frac{T_A}{T}-1-\ln\frac{T_A}{T}\right)$$

$$\ln\frac{\gamma_B^s x_B^s}{\gamma_B^l x_B^l} = -\frac{\Delta H_B}{R}\left(\frac{1}{T_B}-\frac{1}{T}\right)-\frac{\Delta C_B}{R}\left(\frac{T_B}{T}-1-\ln\frac{T_B}{T}\right)$$

where

$$\ln\gamma_A^s = \frac{\Omega_s}{RT}\,(1-x_A^s)^2$$

$$\ln\gamma_A^l = \frac{\Omega_l}{RT}\,(1-x_A^l)^2$$

TABLE 3

Thermodynamic properties of $NaNO_3$ and KNO_3 used for the calculation of the solidus and liquidus of the $NaNO_3$—KNO_3 system

	T_m/K	ΔH_m/kJ mole^{-1}	ΔC_p/J mole^{-1} K^{-1}	Ω_l/kJ mole^{-1}
$NaNO_3$	580 [18]	15.5 [19]	23.0 *	−1.85 **
KNO_3	610 [18]	10.0 [20]	3.8 [20]	

* Calculated from refs. 21 and 22.
** Calculated from ref. 16.

and T_i, ΔH_i, and ΔC_i are the melting temperature, the enthalpy of fusion, and the heat capacity difference between the liquid and the solid for each component, and A and B represent $NaNO_3$ and KNO_3. Ω_l and Ω_s are the interaction parameters in the liquid and in the solid, and γ_i^l and γ_i^s the activity coefficients.

The literature values listed in Table 3 were used for the calculation, and it was performed by the Runge—Kutta—Gill method by changing the value of Ω_s as a parameter. The liquidus and solidus are strongly dependent on the parameter Ω_s, and the minimum melting temperature, 222°C, of this system was given when Ω_s was 6.2 kJ mole^{-1}. The calculated liquidus and solidus for this value are drawn in Fig. 9 by solid lines, which agree well with those measured by other investigators [9,10]. The enthalpy of mixing of the solid solution at $x = 0.5$ is calculated to be 1.6 kJ mole^{-1} from the value of Ω_s.

ΔH^{mix} (s, $x = 0.5$) can also be estimated following the relation shown in Fig. 10 by using the literature values of the enthalpy of fusion and the heat capacity for $NaNO_3$ and KNO_3, such as those listed in Table 3, and the heat capacity of the liquid phase HTS_2 and the enthalpy of fusion of HTS_2 determined in the present study. The estimated value of ΔH^{mix} (s, $x = 0.5$) is 2.81 ±1.34 kJ mole^{-1} which agrees with 1.6 kJ mole^{-1} within experimental error. The positive value of Ω_s calculated is also in accord with the observed phenomenon of the phase separation.

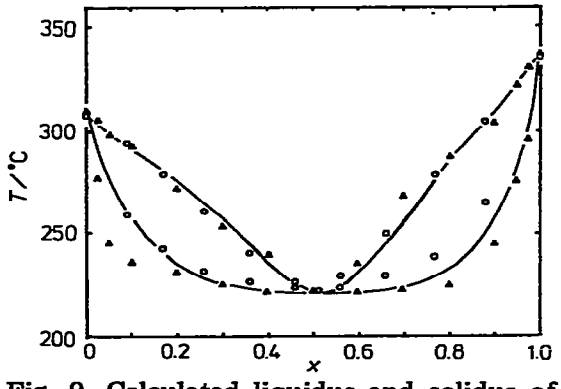

Fig. 9. Calculated liquidus and solidus of the $NaNO_3$—KNO_3 system. ○, Kofler [9]; △, Susarov et al. [10]; ———; calculated.

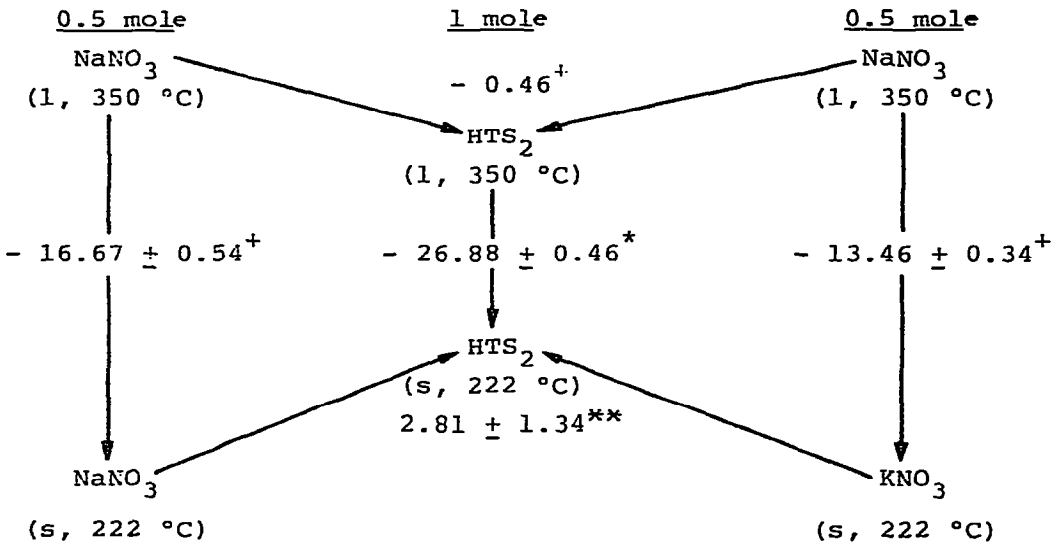

Fig. 10. Enthalpy change relation in the $NaNO_3$—KNO_3 system. †, literature value; *, value obtained in the present study; **, value calculated from other values in the figure. Enthalpy values in kJ.

The consistency in the thermodynamic properties and the phase diagram of this system was thus confirmed. However, the boundary curve of the homogeneous solid phase and the separated solid phases was not calculated because $NaNO_3$ and KNO_3 have different types of phase transitions below the melting temperature and because information on the phase transitions in the solid solution are available only in the limited composition range of this system [23].

CONCLUSION

The mechanism of formation of the solid solution, the phase separation, and the formation of the eutectic mixture were investigated for HTS_2 by DSC and X-ray diffraction. It was shown that the formation of the solid solution below the melting point is rapid and that the phase separation and the formation of the eutectic mixture are influenced by the thermal history of the sample.

The enthalpy change was measured for annealed and quenched samples of HTS_2 from room temperature to 450°C by a high-temperature calorimeter of the twin type. The enthalpy of fusion and the heat capacities of the liquid phase and two stable solid phases were determined.

It was shown that the Kopp—Neumann law roughly holds for the heat capacity of the liquid phase HTS_2. The heat capacity value in the solid II (the quenched phase) averaged between 25 and 100°C was the same as the molar average of the values for $NaNO_3$ and KNO_3.

The liquidus and solidus of the $NaNO_3$—KNO_3 system were calculated from the literature values of the enthalpy of fusion and the heat capacity for $NaNO_3$ and KNO_3 and from the reported enthalpy of mixing in the liquid

for this system assuming the regular solution approximation for the solid solution, where the interaction parameter in the solid was chosen so that the minimum melting temperature of this system becomes 222° C.

The calculated liquidus and solidus are in good agreement with the values measured by other investigators, and the enthalpy of mixing in the solid solution calculated from the interaction parameter chosen was in agreement with that estimated from the reported enthalpy of fusion and heat capacity data for the components and from the enthalpy change data of HTS_2 measured in the present study.

This agreement shows that the data obtained are reliable and that the regular solution approximation for the solid solution is applicable to this system.

ACKNOWLEDGEMENTS

The author would like to express his grateful thanks to Dr. T. Ozawa and Prof. Y. Takahashi for their valuable suggestions and comments. He is also indebted to Mr. N. Umesaki for experimental help in the X-ray diffraction.

REFERENCES

1 S.I. Berul and A.G. Bergman, Izv. Sekt. Fiz. Khim. Anal., Inst. Obshch. Neorg. Khim., Akad. Nauk SSSR, 25 (1954) 233.
2 M.D. Silverman and J.R. Engel, U.S. Dep. Commer. ORNL/TM-5682, 1977.
3 P. Nguyen-Duy and E.A. Dancy, Thermochim. Acta, 39 (1980) 95.
4 N.K. Voskresenskaya, G.N. Yankovskaya and V.Y. Anosov, Zh. Prikl. Khim. (Moscow), 21 (1948) 18.
5 H.V. Venkatesetty and R.T. Lefrois, Proc. 11th Intersoc. Energy Conv. Eng. Conf., 1976, American Institute of Chemical Engineers, p. 606.
6 D.I. Marchidan and C. Telea, Rev. Chim. Acad. Repub. Pop. Roum., 13 (1968) 1291.
7 E. Jänecke, Z. Anorg. Chem., 259 (1949) 92.
8 G. Tamman and A. Ruppelt, Z. Anorg. Chem., 197 (1931) 65.
9 A. Kofler, Monatsh. Chem., 86 (1955) 643.
10 M.P. Susarov, A.I. Efimov and L.S. Timoshenko, Russ. J. Phys. Chem., 43 (1969) 795.
11 M. Kamimoto, Thermochim. Acta 41 (1980) 361.
12 D.A. Ditmars and T.B. Douglas, J. Res. Natl. Bur. Stand. U.S., Sect. A, 75 (1971) 401.
13 C.N.R. Rao, B. Prakash and M. Natarajan, U.S. Dep. Commer., NSRDS-NBS 53, 1975.
14 F. Seitz, The Modern Theory of Solids, McGraw-Hill, New York, 1940, p. 38.
15 H. Miekk-Oja, Ann. Acad. Sci. Fenn., Ser. A, 7 (1941) 46.
16 O.J. Kleppa, J. Phys. Chem., 64 (1960) 1937.
17 G.N. Lewis and M. Randall, Thermodynamics, revised by K.S. Pitzer and L. Brewer, McGraw-Hill, New York, 1961, 2nd edn.,
18 G.J. Janz, C.B. Allen, N.P. Bansal, R.M. Murphy and R.P.T. Tomkins, U.S. Dep. Commer., NSRDS-NBS 61, Part II, 1979.
19 H.M. Goodwin and T.H. Kalmus, Phys. Rev., 28 (1909) 1.
20 R.P. Clark, J. Chem. Eng. Data, 18 (1973) 67.
21 V.C. Reinsborough and F.E.W. Wetmore, Aust. J. Chem. 20 (1967) 1.
22 A.S. Dworkin and M.A. Bredig, J. Phys. Chem., 67 (1963) 697.
23 W. Klement, Jr., J. Inorg. Nucl. Chem., 36 (1974) 1916.